Soliton lattice in superfluid ^{3}He-A

Robijn Bruinsma and Kazumi Maki
Department of Physics, University of Southern California, Los Angeles, California 90007
(Received 11 December 1978)

High-density composite solitons in superfluid ^{3}He-A form a regular one-dimensional lattice. The magnetic-resonance frequencies and the intensities of these soliton lattices are determined theoretically. Furthermore, if the soliton lattice has open ends, the soliton lattice relaxes by uncoiling the $\hat{l}$ and $\hat{d}$ vectors. The characteristic time for the uncoiling is calculated. The present theory appears to account for unusual NMR behavior in magnetization-tipping experiments.

I. INTRODUCTION

In a series of papers Maki and Kumar[1–4] have studied a variety of domain-wall-like textures in superfluid ^{3}He-A. In particular, when the superfluid is confined in a long cylinder with a diameter much larger than the dipole coherence length $\xi_\perp$ ($\simeq 10$ μm), it was shown[2,4] that the most stable domain wall is a twist composite soliton in the presence of an axial magnetic field, while the splay composite soliton has the lowest energy if the magnetic field is perpendicular to the cylinder axis. The existence of the composite solitons, which involve both the $\hat{d}$ vector (describing the spin component of the A-phase order parameter) and the $\hat{l}$ vector (describing the orbital symmetry axis of the order parameter) has been confirmed by Avenal *et al.*[5] and by Gould and Lee[6] through detection of the satellite resonance frequencies in the NMR spectrum of ^{3}He-A. In more recent experiments by Giannetta *et al.*[7] and by Bozler and Bartolac,[8] the magnetization was tipped by a large angle ($\sim 180°$). After the tipping they discovered that the NMR absorption was almost exhausted by the satellite resonance unlike the earlier experiments[5,6] where the Leggett resonance gave the dominant absorption peak. Furthermore Bozler and Bartolac (BB) discovered a time dependence in the NMR satellite frequency. Only a few minutes after the tipping did they observe the NMR consistent with a composite soliton.

The object of the present paper is to study a regular array of composite solitons (i.e., one-dimensional soliton lattice) and their magnetic responses. The work is partially motivated by the puzzling features in the tipping experiments. In the tipping experiments a large number of composite solitons are created. Suppose that all $\hat{d}$ solitons created magnetically decay into composite solitons[9] then the soliton density per unit length is estimated[10] as $N_s \cong (2/\pi)(\omega_0/\Omega_A)\xi_\perp^{-1}$, where ω_0 is the Larmor frequency associated with the static magnetic field H_0, Ω_A is the Leggett frequency, and $\xi_\perp$ is the dipole coherence length (~ 10 μm). For $H_0 \sim 1$ kOe, N_s can be of the order 10^5 cm^{-1} although apparently N_s cannot exceed

$$\xi_0^{-1}(T) \sim 5 \times 10^5 (1 - T/T_c)^{1/2} \text{ cm}^{-1} ,$$

where $\xi_0(T)$ is the temperature-dependent BCS coherence distance. At such a high density, composite solitons are very likely to form a regular array due to their strong mutual repulsion. In particular in the twist case, the regular lattice is an exact solution of the Euler-Lagrange equation for the textures. Then the spin-wave spectrum is quite different from that for an isolated soliton. In particular we can interpret the time dependence of the satellite frequency as due to the time dependence of the soliton density. Furthermore we show that the NMR absorption is dominated by the satellite resonance for a soliton density $N_s > 10^{-1}\xi_\perp^{-1}$ ($\sim 10^2$ cm^{-1}), which is again consistent with the tipping experiment by Bozler and Bartolac.[8]

In Sec. II we shall study the regular soliton lattice for both twist and splay cases. In Sec. III we calculate the spin-wave spectra for those two soliton lattices and their relative intensities in the NMR absorption. Section IV is devoted to the relaxation of the solition lattice due to the orbital relaxation. It is shown that in usual circumstances the soliton density decreases exponentially in time. The characteristic time is of the order of 10 minutes for the twist case and of the order of a few minutes for the splay case.

II. SOLITON LATTICE

The order parameter of superfluid ^{3}He-A is given by a 3×3 matrix $A_{\mu i} = \hat{d}_\mu \vec{\Delta}_i$. Here d is a real unit vector describing the spin component and $\vec{\Delta}$ is a complex vector describing the orbital component; $\vec{\Delta} = [1/(2)^{1/2}]\Delta_0(T)(\hat{\delta}_1 + i\hat{\delta}_2)$, where $\hat{\delta}_1$, $\hat{\delta}_2$, and $\hat{l}(\equiv \hat{\delta}_1 \times \hat{\delta}_2)$ form a triad of unit vectors. $\Delta_0(T)$ is the temperature-dependent amplitude of the order parameter.

The free energy corresponding to inhomogeneous

textures is given in the Ginzburg-Landau regime by[2]

$$F_{\rm kin}=\tfrac{1}{2}K\int d^3r\,\{3|\vec{\nabla}\cdot\vec{\Delta}|^2+|\vec{\nabla}\times\vec{\Delta}|^2+2|\vec{\Delta}\cdot\vec{\nabla}\hat{d}|^2 +|\vec{\Delta}|^2[|\vec{\nabla}\cdot\hat{d}|^2+(\vec{\nabla}\times\hat{d})^2]\}\ , \quad (1)$$

where

$$K=\frac{6}{5}\left(\frac{N}{8m^*}\right)\frac{7\zeta(3)}{(2\pi T_c)^2}$$

for the weak-coupling model. To this should be added the nuclear dipole energy

$$E_D=-\tfrac{1}{2}\chi_N\Omega_A^2\int d^3r\,(\hat{l}\cdot\hat{d})^2\ , \quad (2)$$

where χ_N is the normal spin susceptibility. In the presence of a strong magnetic field along the z direction, $\hat{l}$ and $\hat{d}$ will be restricted to the x-y plane

$$\hat{d}=\sin\psi\hat{x}+\cos\psi\hat{y}\ ,$$

$$\hat{l}=\sin\chi\hat{x}+\cos\chi\hat{y}\ ,$$

and

$$\vec{\Delta}=(2)^{-1/2}\Delta_0 e^{i\phi}(-\cos\chi\hat{x}+\sin\chi\hat{y}+i\hat{z})\ . \quad (3)$$

Furthermore, in the case of domain walls ψ and χ will depend only on $s=\hat{n}\cdot\vec{x}$, where $\hat{n}\equiv(n_1,n_2,n_3)$ is a unit vector normal to the domain wall and parallel to the cylinder axis. The free energy per unit surface (normal to $\hat{n}$) f of the system becomes

$$f=\frac{F}{\sigma}=\tfrac{1}{2}A\int ds\left\{\left[1+2a^2\left(1-\frac{n_3^2}{2-a^2}\right)\right]\chi_s^2+2(2-a^2)\times\psi_s^2+4\xi_\perp^{-2}\sin^2(\chi-\psi)\right\}\ , \quad (4)$$

where $A=\frac{1}{2}K\Delta_0^2$ and $a=n_1\sin\chi+n_2\cos\chi$, the suffix s implies the derivative with respect to s, and σ is the surface area of the domain wall. The phase $\phi(s)$ has been eliminated. In the following we limit ourselves to two cases.

A. Twist solitons

When the magnetic field is in the axial direction, we have $\vec{n}=\hat{z}$. Then, introducing new variables by

$$u=\chi+4\psi\ ,\quad v=\chi-\psi\ , \quad (5)$$

we have

$$f=\tfrac{1}{2}A\int ds\,(\tfrac{1}{5}u_s^2+\tfrac{4}{5}v_s^2+4\xi_\perp^{-2}\sin^2 v)\ . \quad (6)$$

A constant u minimizes f. We take hereafter $u=0$. Minimizing f with respect to v gives

$$\tfrac{2}{5}v_{ss}-\xi_\perp^{-2}\sin 2v=0\ . \quad (7)$$

The only stable periodic solution of this equation is[11]

$$\cos v=\mathrm{sn}\left(\frac{(5)^{1/2}}{k\xi_\perp}s\,|k\right)\ , \quad (8)$$

where sn is a Jacobian elliptic function[12] of parameter $m=k^2$. Equation (8) describes a regular soliton lattice with a lattice constant

$$L_0=\frac{2}{(5)^{1/2}}\xi_\perp kK(k)\ , \quad (9)$$

where $K(k)$ is a complete elliptic integral of the first kind. In the limit $k\to 0$, Eq. (8) becomes

$$\cos v=\sin\left(\frac{(5)^{1/2}}{k\xi_\perp}s\right)\ .$$

$\hat{l}$ and $\hat{d}$ rotate in the opposite direction at a constant rate around the z axis forming a double helix. This is shown schematically in Fig. 1(a). In the opposite limit $k\to 1$, we have

$$\cos v=\tanh\left(\frac{(5)^{1/2}}{\xi_\perp}s\right)\ ,$$

which describes an isolated soliton.

Substituting Eq. (8) into the expression for the free energy, we find

$$f=2A\,\xi_\perp^{-2}m^{-1}\{2[E(k)/K(k)]-m_1\}\ , \quad (10)$$

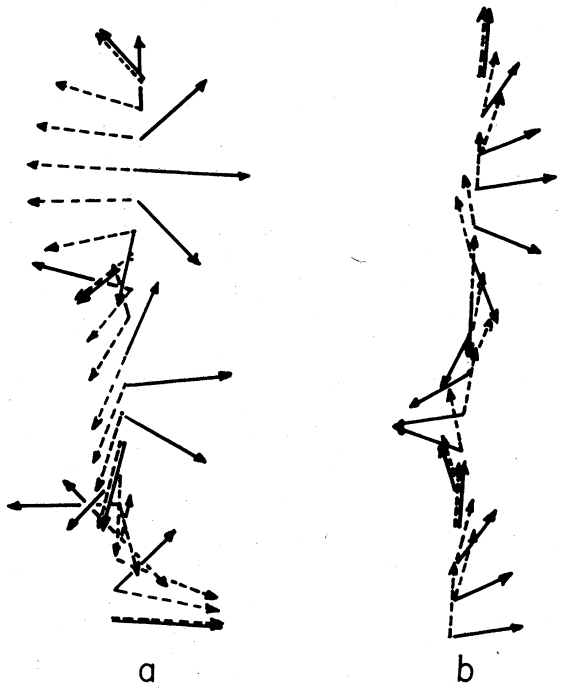

FIG. 1. Soliton lattices for the twist case (a) and the splay case (b) are shown schematically. The solid arrow indicates the direction of the $\hat{l}$ vectors, while the broken arrow indicates that of the $\hat{d}$ vector.

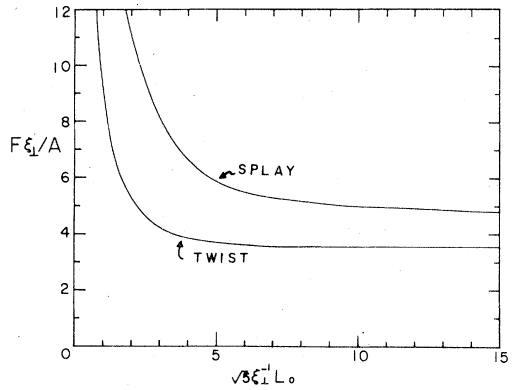

FIG. 2. Free energies per unit soliton distance L_0 are shown for the twist case and the splay case.

where $m=k^2$, $m_1=1-m$, and $E(k)$ is a complete elliptic integral of the second kind. Here f is the free energy per unit length. f decreases monotonically as L_0 increases as shown in Fig. 2. As $L_0\to\infty$, f goes to the previously obtained limit for a single soliton[2] (per length L_0),

$$f|_{L_0=\infty}=\frac{8}{(5)^{1/2}}A(\xi_\perp L_0)^{-1}\ . \tag{11}$$

B. Splay soliton

We now consider the case where H_0 is applied perpendicular to the cylinder axis. We then take $\hat{n}=\hat{y}$. For this case the exact solution is rather difficult to obtain, as χ and ψ are coupled. Therefore we shall look for a variational solution of the form

$$\cos\chi=\mathrm{sn}(\lambda s|k)\ ,\quad \sin\psi=\alpha\,\mathrm{cn}(\lambda s|k)\,\mathrm{sn}(\lambda s|k)\ , \tag{12}$$

where α and λ are variation parameters. We shall determine α and λ so that the free energy has a minimum for a given spacing between two solitons; the free energy is minimized with the condition

$$L_0=2K(k)\lambda^{-1}\ , \tag{13}$$

where L_0 is the soliton lattice constant. The solution is schematically shown in Fib. 1(b). The present solution does not approach the splay composite soliton solution[4] in the limit $k\to 1$, as the $\hat{l}$ vector is held asymptotically parallel or antiparallel to $\hat{n}$. Therefore, the solution considered here is rather close to a regular array of $\hat{l}$ textures.[3] However, we believe that the present solution is reasonable as long as the soliton spacing L_0 is not much larger than $\xi_\perp$ (say $L_0\leq 10\xi_\perp$), which region is of prime interest. Furthermore, as noted already the satellite frequencies associated with the splay composite soliton are rather close to those for the splay $\hat{l}$ textures. We have substituted Eq. (12) into Eq. (4) and minimized f with respect to λ and α for fixed L_0. The result is shown in Fig. 2. In the limit of large L_0 we obtain

$$f=4.802A(\xi_\perp L_0)^{-1}\ ,\quad \text{with } \alpha=0.481\ . \tag{14}$$

For $L_0\geq 10\xi_\perp$, f will reduce this value gradually to $f=4.0A(\xi_\perp L_0)^{-1}$, as the asymptotic $\hat{l}$ direction far from the soliton relaxes from parallel to $\vec{v}_s$ to that of the splay composite soliton.

In the other limit $L_0\ll\xi_\perp$ we find

$$f=9.56AL_0^{-2}\ ,\quad \text{with } \alpha=0\ . \tag{15}$$

For intermediate values of L_0, we give a table of m and α values, which minimize f, as a function of $L_0/\xi_\perp$ (Table I).

We see from the present analysis that f diverges like L_0^{-2} for small L_0 (i.e., $L_0/\xi_\perp\ll 1$), while it approaches an asymptotic value proportional to L_0^{-1} in the limit of large separation. The solitons act as particles with a strong repulsive interaction potential with a range of roughly $10\xi_\perp$.

TABLE I. α, $K(k)$, λ_f, and λ_g for the splay soliton lattice are given as functions of $L_0/\xi_\perp$.

L_0/ξ	α	$K(k)$	λ_f	λ_g
0	0	1.98	0.080	0.550
1	0.030	2.05	0.146	0.573
2	0.108	2.31	0.210	0.601
3	0.200	2.60	0.276	0.638
4	0.290	3.03	0.327	0.665
5	0.352	3.42	0.350	0.685
6	0.400	3.84	0.364	0.696
7	0.433	4.34	0.369	0.708
8	0.455	4.82	0.368	0.709
9	0.471	5.39	0.368	0.710
10	0.480	5.90	0.365	0.710

III. MAGNETIC RESONANCE

The magnetic resonance has proved to give a detailed insight in the dipole generated textures like composite solitons. In response to an external rf field the $\hat{d}$ vector oscillates in the potential provided by the local $\hat{l}$ vector. In general spin-wave modes can be localized as well as extended. For example the Leggett resonance in the bulk liquid arises from an extended mode, while satellite resonances are due to localized modes (the spin-wave bound state trapped at the dipole potential due to the texture). In the case of a soliton lattice, the spin-wave spectrum has a band structure. Then the rf field couples to the spin wave with a particular wave vector q. Hence the NMR experiment allows one to explore a small portion of the spin-wave band structure.

To determine the resonance frequencies we parametrize the $\hat{d}$ vector as[2]

$$\hat{d}=\cos g[\sin(\psi+f)\hat{x}+\cos(\psi+f)\hat{y}]+\sin g\hat{z}\ , \tag{16}$$

where ψ describes the equilibrium $\hat{d}$ configuration and f and g describe small oscillations. Substituting Eq. (16) into Eq. (1), we construct a set of eigen equations for f and g. Then the NMR frequencies are given in terms of these eigenvalues,[2] while the intensities of the resonances are calculated from the eigenfunctions. To do this we first note that the magnetization associated with the $\hat{d}$ oscillation is given by[2]

$$\vec{M}=-\gamma_0 X_N(-\sin\psi g_t\ ,\ \cos\psi g_t\ ,\ f_t)\ , \tag{17}$$

where suffices t imply the time derivative. Then the intensities of the longitudinal and the transverse resonance are given by[13]

$$I_l^{(n)}=\left|\int_{-\infty}^{\infty} f_n(s)\,ds\right|^2$$

and

$$I_t^{(n)}=\left|\int_{-\infty}^{\infty} g_n(s)\sin\psi(s)\,ds\right|^2 + \left|\int_{-\infty}^{\infty} g_n(s)\cos\psi(s)\,ds\right|^2 , \tag{18}$$

where $f_n(s)$ and $g_n(s)$ are the normalized nth eigenfunctions. Furthermore from the closure properties of $\{g_n(s)\}$ and $\{f_n(s)\}$, the sum of the intensities has to be unity

$$\sum_n I_l^{(n)}=1\ ,\quad \sum_n I_t^{(n)}=1\ . \tag{19}$$

A. Twist soliton lattice

Again we shall consider the twist case and the splay case separately. The fluctuation free energy δf is given by

$$\delta f=2A\int ds\,\{(f_s^2+g_s^2)+\xi_\perp^{-2}\cos[2(\chi-\psi)]f^2 + [\xi_\perp^{-2}\cos^2(\chi-\psi)-\psi_s^2]g^2\}\ , \tag{20}$$

where we have retained only the quadratic terms in f and g. Then the eigenvalue equations are given by

$$\lambda_f f=-\xi_\perp^2 f_{ss}+\cos[2(\chi-\psi)]f\ , \tag{21}$$

$$\lambda_g g=-\xi_\perp^2 g_{ss}+[\cos^2(\chi-\psi)-\xi_\perp^2\psi_s^2]g\ , \tag{22}$$

while the resonance frequencies are given by

$$\omega_l=(\lambda_f)^{1/2}\Omega_A\ ,\qquad \omega_t^2=\omega_0^2+\lambda_g\Omega_A^2\ , \tag{23}$$

for the longitudinal and transverse resonance, respectively.

First let us consider the longitudinal resonance [Eq. (21)], where $\chi-\psi=v$ is given by Eq. (8). In the limit $k\to 0$ (i.e., $L_0/\xi \ll 1$), the potential is given by $\cos[2(\chi-\psi)]=2\sin^2[(5)^{1/2}\xi_\perp^{-1}z]$ and Eq. (21) reduces to a Mathieu equation. Furthermore the longitudinal resonance picks up the spin-wave mode with $q=0$ (zero wave vector). In fact, in this limit, the only eigenmode, which couples to the rf field is $e_0(z)\ \{=1-\frac{1}{5}\cos[2(5)^{1/2}\xi_\perp^{-1}x]+\cdots\}$, which yields $\lambda_f=0$ to leading order.

In the other limit $L_0/\xi_\perp \gg 1$, where k tends to 1 we recover the solution associated with an isolated soliton

$$\lambda_f f=-\xi_\perp^2 f_{zz}+\{1-2\,\mathrm{sech}^2[(5)^{1/2}\xi_\perp^{-1}z]\}f\ , \tag{24}$$

with

$$f\propto\{\mathrm{sech}[(5)^{1/2}\xi_\perp^{-1}z]\}^{[(13/5)^{1/2}-1]/2}$$

and

$$\lambda_f=\tfrac{1}{2}[(65)^{1/2}-7]\ . \tag{25}$$

Furthermore, in this limit there are a set of scattering states with λ_f slightly larger than unity, which do contribute to the longitudinal resonance.

For intermediate values of $L_0/\xi_\perp$, we shall determine the eigenvalue variationally. For the bound state (i.e., the state with $\lambda_f<1$), we make use of a variational function

$$f\propto \mathrm{dn}^\nu[(5)^{1/2}\xi_\perp^{-1}z\,|k]\ , \tag{26}$$

with ν as a variational parameter. Here dn is a Jacobian elliptic function. Equation (26) interpolates the two limiting solutions nicely. Then λ_f is determined by

$$\lambda_f=\frac{\int_0^{L_0} ds\,[5\nu^2\,\mathrm{cn}^2\,\mathrm{sn}^2\,\mathrm{dn}^{2\nu-2}+(2\,\mathrm{sn}^2-1)\,\mathrm{dn}^{2\nu}]}{\int_0^{L_0} ds\,\mathrm{dn}^{2\nu}}\ , \tag{27}$$

where all elliptic functions have $(5)^{1/2}\xi_\perp^{-1}z$ as argument and k^2 as parameter. In the limit $k \to 0$ and $k \to 1$, we can work out the integral analytically and we find

$$\lambda_f = 0.1k^2 , \quad \text{with } \nu = 0.2$$

for $k \to 0$, for example.

For general k, Eq. (27) is evaluated numerically and then minimized with respect to ν. The general result is shown in Fig. 3. We have also calculated the intensity from Eq. (18) and it is shown in Fig. 4. λ_f increases from zero as the lattice spacing increases and reaches the value for the isolated soliton when $L_0 \simeq 8\xi_\perp$. On the other hand for small L_0, the intensity is completely exhausted by the bound state. Only for $L_0 > 8\xi_\perp$ does the intensity of the satellite peak begin to decline. For larger L_0 (i.e., $L_0 >> \xi_\perp$), the intensity decreases like $I_l^{(b)} \simeq 6.04(\xi_\perp/L_0)$.

For large separation ($L_0 >> \xi_\perp$), the scattering states for Eq. (24) can be constructed as the exact scattering matrix is known. When the potential in Eq. (24) is arranged in a linear array with a distance L_0, the spin-wave function takes the form

$$f(z) = e^{iqz}u_z(z) ,$$

with

$$u_z(z + L_0) = u_q(z) . \tag{28}$$

Then $u_z(z)$ is very well approximated for small q by (for derivation see Appendix A)

$$u_q(z) \simeq \sin\left[\pi M\left(\frac{z - \frac{1}{2}\delta_l}{L_0 - \delta_l}\right)\right] , \quad \text{for } 0 < z < L_0 , \tag{29}$$

where solitons are assumed to be located at $z = 0$, $\pm L_0$, etc. Here M is an integer and δ_l is given

$$\delta_l = \frac{1}{(5)^{1/2}}\xi_\perp[\psi(1+\sigma) + \psi(-\sigma) + 2\gamma - \Gamma(-\sigma)\Gamma(1+\sigma)] = 6.04\xi \tag{30}$$

and $\sigma = \frac{1}{2}[(\frac{13}{5})^{1/2} - 1]$. $\Gamma(z)$ and $\psi(z)$ are the γ and the digamma function, and $\gamma \simeq 1.76$ is the Euler constant.

Furthermore, it is easily seen that only the scattering states with $q = 0$ and odd M couple to the longitudinal rf field. The longitudinal resonance frequencies are given then by

$$\lambda_f^{(n)} = 1 + (2n+1)^2\pi^2\left(\frac{\xi_\perp}{L_0 - \delta_l}\right)^2 , \tag{31}$$

with intensities

$$I_l^{(n)} \cong \frac{8}{(2n+1)^2\pi^2}\left(1 - 6.04\,\frac{\xi_\perp}{L_0}\right) , \tag{32}$$

with $n = 1, 2, \ldots$.

Therefore for $L_0 >> \xi_\perp$, there is an infinite series of scattering states, which contribute to the longitudinal resonance. All these resonance frequencies reduce to the Leggett frequency as L_0 becomes much larger than $\xi_\perp$. $\lambda_f^{(n)}$ for $n = 0, 1, 2$ is shown as a function of L_0 in Fig. 5, while the intensities for $n = 0$, 1, and 2 are shown in Fig. 4.

Now turning to the transverse resonance, the rf field couples to the spin-wave modes with $q = (2\pi/5L_0)j$ ($j = 1, 2, \ldots$), since $\sin\psi(z)$ and $\cos\psi(z)$ have a period of $5L_0$. First, the bound spin wave is determined by making use of the following variational function $g \propto e^{iqz}\mathrm{dn}^\mu[(5)^{1/2}\xi^{-1}z|k]$, with μ as a variational parameter. As in the case of the longitudinal resonance, the above function interpolates two limiting exact results for $k \to 0$ and $k \to 1$. The result for $\lambda_g^{(b)}$ is shown as a function of L_0 in

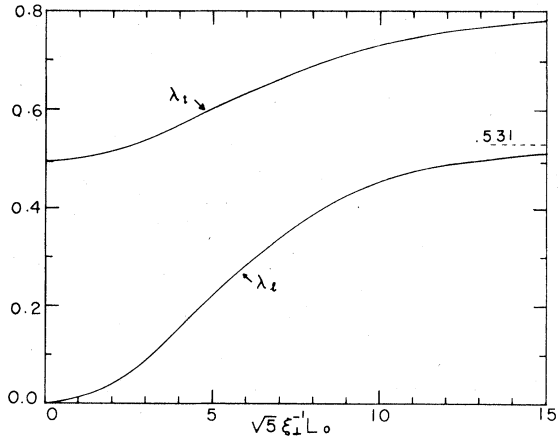

FIG. 3. λ_t ($\equiv\lambda_g$) and λ_l ($\equiv\lambda_f$), which appear in the transverse and the longitudinal satellite frequency, are shown as functions of soliton separation L_0 for the twist case.

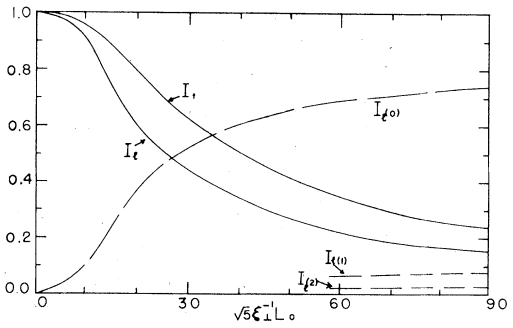

FIG. 4. Intensities of the longitudinal satellite I_l and of the transverse satellite I_t are shown as functions of L_0. $I_l^{(0)}$, $I_l^{(1)}$, and $I_l^{(2)}$ are the intensities from the scattering states in the longitudinal resonance.

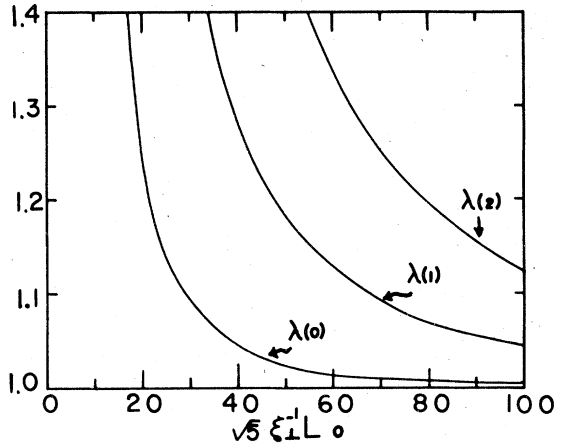

FIG. 5. $\lambda_l^{(n)}$ associated with the longitudinal scattering states are shown as functions of L_0.

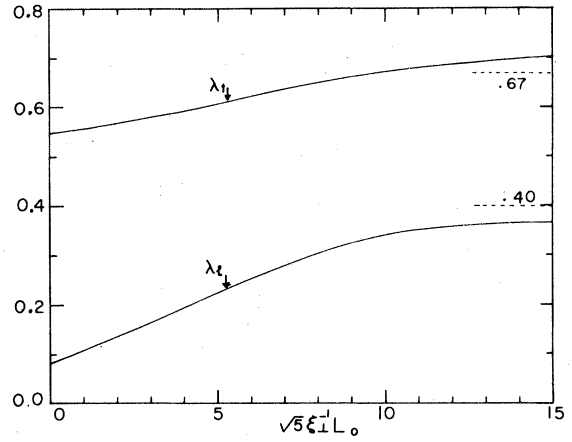

FIG. 6. λ_t ($\equiv\lambda_g$) and λ_l ($\equiv\lambda_f$) for the splay soliton lattice are shown as functions of L_0.

Fig. 3 together with $\lambda_f^{(b)}$. λ_g increases monotonically from 0.5 for $L_0=0$ to 0.8 as L_0 increases. Furthermore, making use of Eq. (18), we have calculated I_t, which is shown in Fig. 4. As in the case of the longitudinal resonance, the bound state almost exhausts the transverse resonance as long as $L_0 \lesssim 10\xi_\perp$. When $L_0 \gtrsim 10\xi_\perp$ there appear intensities associated with the scattering states. The scattering states are handled similarly when $L_0 \gtrsim 10\xi_\perp$. We now find

$$\lambda_g^{(n)} = 1 + [(2n+1)^2 + \tfrac{1}{25}]\pi^2\left(\frac{\xi_\perp}{L_0 - \delta_t}\right)^2 \tag{33}$$

and

$$I_t^{(n)} = [1-\cos(\tfrac{4}{5}\pi)][(2n+\tfrac{6}{5})^{-1} + (2n+\tfrac{4}{5})^{-1}]^2 \times \pi^2\left[1 - O\left(\frac{\xi_\perp}{L}\right)\right], \tag{34}$$

with $n=0,1,\ldots,$ where

$$\delta_t = (5)^{-1/2}\xi_\perp[2\gamma + \psi(1+\delta') + \psi(-\sigma') - \Gamma(-\sigma')\Gamma(1+\sigma')] \tag{35}$$

and $\sigma' = \frac{1}{5}$.

B. Splay soliton lattice

For the splay solution lattice, we obtain eigen equations

$$\lambda_f f = -\tfrac{1}{2}\xi_\perp^2 \frac{d}{ds}[(1+\sin^2\chi)f_s] + [1-2\sin^2(\chi-\psi)]f\,,$$

$$\lambda_g g = -\tfrac{1}{2}\xi_\perp^2 \frac{d}{ds}[(1+\sin^2\chi)g_s] + [1-\sin^2(\chi-\psi) - \tfrac{1}{2}(1+\sin^2\chi)\xi_\perp^2\psi_s^2]g\,, \tag{36}$$

where χ and ψ are given in Eq. (12) and f and g describe the $\hat{d}$ oscillation as given in Eq. (16). In the present case, no exact result is known even in the limiting situations. Therefore we determine the bound-state eigenvalues variationally by assuming that $f \propto [\mathrm{ds}(\lambda s|k)]^\nu$ and $g \propto [\mathrm{dn}(\lambda s|k)]^\mu$ where dn is a Jacobian elliptic function and λ and k correspond to the equilibrium solution. Note that in the present situation both the longitudinal and the transverse rf field couples with the spin-wave mode with $q=0$ (zero wave vector). The result of the variational calculation is shown in Fig. 6. λ_f increases from 0.083 to 0.366 as L_0 increases from 0 to 10 $\xi_\perp$, while λ_g increases from 0.550 to 0.707. Both λ_f and λ_g saturate around $L_0 \simeq 10\xi_\perp$. The broken lines in the figure are the values expected for an isolated splay composite soliton[4,14] ($\lambda_f=0.40$ and $\lambda_g=0.670$).

Small discrepancies in the asymptotic values are due to the fact that our equilibrium solution Eq. (12) does not have appropriate asymptotic behavior for $L_0 >> \xi_\perp$. However, as already explained, we believe our variational solution is reliable for $L_0 \lesssim 10\xi_\perp$. We have also calculated the intensities of these modes, which are shown in Fig. 7. As in the twist case, the

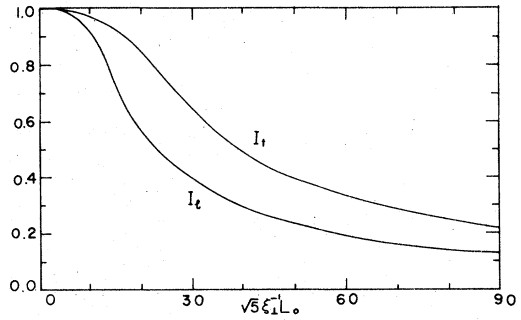

FIG. 7. Intensities I_l and I_t are shown as functions of L_0.

bound states appear to exhaust the resonance for $L_0 \lesssim 10\xi_\perp$. For $L_0 > 10\xi_\perp$ the intensities associated with the scattering states with resonance frequency slightly above the Leggett frequency become more and more important. The λ_f's and λ_g's associated with the scattering states are given by

$$\lambda_f^{(n)} = 1 + (2n+1)^2\pi^2\left(\frac{\xi_\perp}{L_0 - \delta_l}\right)^2$$

and

$$\lambda_g^{(n)} = 1 + (2n+1)^2\pi^2\left(\frac{\xi_\perp}{L_0 - \delta_t}\right)^2 , \tag{37}$$

with

$$\delta_l = 5.15\xi_\perp , \quad \delta_t = 7.2\xi_\perp ,$$

where δ_l and δ_t have been determined using our sum rule Eq. (19).

The present result for the transverse resonance is of particular interest, in view of the recent tipping experiment by Bozler *et al.*[8] The experiment was done in the splay configuration. Immediately after the magnetization was tipped by large angle, Bozler *et al.* observed a clear resonance with a negative shift, which is consistent with the Brinkman-Smith[15] picture of a rotating $\hat{d}$ vector in the x-y plane. However, this negatively shifted resonance was eaten up rapidly on the order of msec. Simultaneously a new resonance appeared with increasing intensity around $\omega \simeq \omega_0 + 0.55\Omega_A^2/2\omega_0$. This new resonance soon exhausted the total absorption. Then the resonance frequency moved gradually upwards and ended up with the frequency expected for the splay composite soliton in a matter of several minutes. If we assume that after the tipping, the Brinkman-Smith oscillation decayed into a highly compressed soliton lattice and that afterwards the soliton lattice relaxed slowly (i.e., the lattice spacing increases gradually) then the present calculation describes quite nicely the above experiment. Furthermore, the calculation does show that the satellite resonance exhausts the total absorption when $L_0 < 10\xi_\perp$. However, if the experiment is performed over a longer time scale then the theory predicts the appearance of a series of resonances with frequency slightly above the Leggett resonance. In Sec. IV, we study a possible soliton lattice relaxation mechanism.

IV. SOLITON LATTICE RELAXATION

After a soliton lattice is created by magnetization tipping in a cylinder with open ends, the soliton density will decrease steadily due to their mutual repulsion. In this circumstance the $\hat{l}$ and $\hat{d}$ vectors at the end points unwind and the soliton density in the cylinder may decrease uniformly, if the uncoiling proceeds rather slowly. Except in the immediate vicinity of the transition temperature, this unwinding process is controlled by the orbital viscosity. In particular, in our parameterization, orbital relaxation is described by

$$-\mu\frac{\partial}{\partial t}\chi = \frac{\delta}{\delta\chi}F(\chi,\psi) , \tag{38}$$

where $F(\chi,\psi)$ is the free energy and μ is the orbital viscosity introduced by Cross and Anderson.[16] For simplicity we consider here the twist soliton lattice. Furthermore, we assume that the soliton lattice relaxes uniformly so that only the soliton spacing L_0 (or k) changes as a function of time. This assumption is justified *a posteriori* as the relaxation proceeds extremely slowly. We can then rewrite Eq. (38) as[17]

$$-\mu m_t\int_0^a\left(\frac{\partial\chi}{\partial m}\right)^2 ds = \frac{\partial}{\partial m}\int_0^a f(\chi,\psi)\,ds , \tag{39}$$

where $m = k^2$, a is the length of the soliton lattice and

$$\cos\chi = \mathrm{sn}[(5)^{1/2}(k\xi_\perp)^{-1}s\,|\,k] . \tag{40}$$

Substituting Eq. (40) into Eq. (39), we obtain after lengthy but straightforward calculation

$$(L_0)_t = \tau^{*-1}L_0 , \tag{41}$$

where $\tau^* = \frac{16}{15}(a/\xi_\perp)^2\tau$, $L_0 = [2/(5)^{1/2}]\xi_\perp kK(k)$, and $\tau = \mu\xi_\perp^2/4A$ is the $\hat{l}$ vector relaxation time in a uniform system as measured by Paulson, Krusius, and Wheatley[18] ($\tau = t_{1/2}/\ln 2$). Finally Eq. (41) is integrated as

$$L_0(t) = L_0(0)\,e^{t/\tau^*} ; \tag{42}$$

the spacing increases exponentially with time or the soliton density $N_s(t)$ $[=N_s(0)e^{-t/\tau^*}]$ decreases exponentially in time. The soliton distribution appears to obey the ordinary diffusion law in a one-dimensional system. The characteristic time depends quadratically on the total length of the soliton lattice. When $a \simeq 1$ cm, we have $\tau^* \cong 10^4(1 - T/T_c)^{1/2}$ sec, where we inserted the observed τ near the melting pressure. Therefore the characteristic time of the soliton lattice with $a \sim 1$ cm is of the order of ten minutes to one hour.

In the case of the splay soliton lattice, the corresponding equation is more complicated and can only be solved numerically. However, in the limit $L_0/\xi_\perp \ll 1$ and $L_0/\xi_\perp \gg 1$, the soliton density is shown to decrease exponentially in time. The characteristic time for the first limit is about $\tau^* = 7a^2(1 - T/T_c)^{1/2}$ and $4a^2(1 - T/T_c)^{1/2}$ min in the second limit at 29 bar. (Here a is measured in cm.) The substantial decrease in the characteristic time in

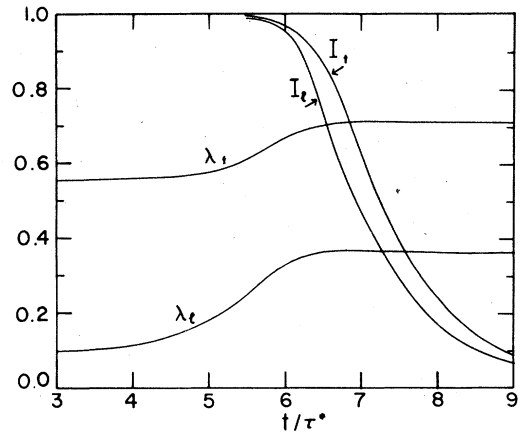

FIG. 8. Time dependence of satellite frequencies and their intensities are shown for the splay soliton lattice. The soliton spacing is assumed to expand exponentially in time.

the case of the splay soliton lattice is due to the steeper slope of the free energy and to the smaller inertial term. The above time scale appears to be again consistent with the experiment.[8] In any case, assuming the exponential decay of the soliton density, the satellite frequencies and their intensities for the splay lattice are plotted as a function of time in an arbitrary unit τ^* in Fig. 8. When more data become available as to the time dependence of the satellite frequencies as well as their intensities, it is hoped that the present prediction can be tested experimentally. The soliton lattice may also be relevant in the turn off experiment by Krusius *et al.*,[19] where they observed rather long $\hat{l}$-field relaxation time.

V. CONCLUSION

We have extended the study of composite solitons in ^{3}He-A to the case of regular soliton lattices. The soliton lattices appear to be realized after the magnetization was tipped by a large angle ($\sim 180°$). We have found equilibrium solutions for given soliton densities both for the twist case and the splay case. In the former case the exact solution is obtained by integrating the Euler-Lagrange equation, while in the latter case the solution is determined variationally. The spin-wave spectra for the soliton lattice have been determined. Furthermore, within the simplest assumption, we find that the soliton density decreases exponentially in time. The soliton lattice, relaxing slowly in time, then accounts for two puzzling features of the magnetic tipping experiment: the time dependence of the satellite frequency and its intensity. This result is quite encouraging, although certainly more experimental work on this subject is desirable.

ACKNOWLEDGMENTS

We thank Hans Bozler and Tom Bartolac for stimulating discussions on their data of the magnetization tipping experiment, which gave the initial impetus to the present study. This work is supported in part by the NSF under Grant No. DMR76-21032.

APPENDIX: SCATTERING STATES FOR A SOLITON LATTICE

We shall determine here the energy spectrum of the eigen equation

$$-\frac{\partial^2}{\partial z^2}\psi(z)+v(z)\psi(z)=E\psi(z)\ , \tag{A1}$$

where $v(z)$ is given by

$$v(z)=\sum_{n=-\infty}^{\infty} V(z+nL_0) \tag{A2}$$

and $V(z)=V(-z)$.

Furthermore we assume that the scattering matrix associated with $V(z)$ is known. For

$$\psi = Ae^{ikz}+Be^{-ikz},\ \text{for } z\to-\infty\ (\text{with } E=k^2) \tag{A3}$$

we have

$$\psi = Fe^{ikz}+Ge^{-ikz}\ ,\ \text{for } z\to+\infty\ , \tag{A4}$$

where

$$\begin{pmatrix}F\\G\end{pmatrix}=\begin{pmatrix}\alpha_1+i\beta_1 & i\beta_2\\ -i\beta_2 & \alpha_1-i\beta_1\end{pmatrix}\begin{pmatrix}A\\G\end{pmatrix}. \tag{A5}$$

Then the solution of Eq. (A1) is written[20]

$$\psi(z)=e^{iqz}u_q(z)\ ,\ \text{with } u_q(z+L_0)=u_q(z) \tag{A6}$$

and q and k are related by

$$\cos qL_0=\alpha_1\cos kL_0+\beta_1\sin kL_0\ . \tag{A7}$$

For definiteness let us consider the longitudinal resonance. In this case the rf field couples only with $q=0$ mode. Furthermore in the case of the twist lattice, where $V(z)=V_0\,\mathrm{sech}^2(\alpha z)$, α_1 and β_1 are given exactly by[21]

$$\alpha_1+i\beta_1=\frac{\Gamma(-ik')\Gamma(1-ik')}{\Gamma(-ik'-\sigma)\Gamma(-ik'+\sigma+1)}\ , \tag{A8}$$

where

$$k'=k/\alpha\ ,\quad \sigma=\tfrac{1}{2}[-1+(1-4\alpha^{-2}V_0)^{1/2}]\ .$$

We are interested in solutions in the limit $L_0/\xi \gg 1$. In this limit we can assume $k' \ll 1$ and

we have

$$\alpha_1 = \frac{1}{\Gamma(1+\sigma)\Gamma(-\sigma)} [2\psi(0) - \psi(\sigma) - \psi(\sigma+1)]$$

and

$$\beta_1 = \frac{1}{k'} \frac{1}{\Gamma(1+\sigma)\Gamma(-\sigma)} + O(k') \ . \tag{A9}$$

Substituting Eq. (A9) into Eq. (A7) we have

$$k(L_0 - \delta_l) = m\pi \ , \tag{A10}$$

where m is an integer and δ_l given in Eq. (30) in the text. The wave function outside of the potential well is approximately given by

$$\psi(z) = A_1 \sin\left(\frac{m\pi z}{L_0 - \delta_l}\right) + B_1 \cos\left(\frac{m\pi z}{L_0 - \delta_l}\right) \tag{A11}$$

for $0 < z < L_0$. However the one which couples to the rf field is given by

$$\psi(z) = A \sin\left(\frac{m\pi(z - \frac{1}{2}\delta_l)}{L_0 - \delta_l}\right), \quad \text{for } 0 < z < L_0 \tag{A12}$$

with odd integer m.

[1]K. Maki and P. Kumar, Phys. Rev. B 14, 118 (1976).

[2]K. Maki and P. Kumar, Phys. Rev. Lett. 38, 577 (1977); Phys. Rev. B 16, 182 (1977).

[3]K. Maki and P. Kumar, Phys. Rev. B 16, 174 (1977).

[4]K. Maki and P. Kumar, Phys. Rev. B 17, 1088 (1978).

[5]O. Avenal, M. E. Bernier, E. J. Varoquaux, and C. Vibet, in *Proceeding of the XIV International Conference on Low Temperature Physics, Otaniemi, Finland, 1975,* edited by M. Krusius and M. Vuorio (North-Holland, Amsterdam, 1955), Vol. 5, p. 429.

[6]C. M. Gould and D. M. Lee, Phys. Rev. Lett. 37, 1223 (1976).

[7]R. W. Giannetta, C. M. Gould, E. N. Smith, and D. M. Lee, in *Quantum Fluids and Solids,* edited by S. B. Trickey, E. D. Adams, and J. W. Dufty (Plenum, New York, 1977).

[8]H. M. Bozler and T. Bartolac, in *Physics of Ultralow Temperatures,* edited by T. Sugawara *et al.* (Physics Society of Japan, Tokyo, 1978); and unpublished.

[9]In this process the $\hat{l}$ vector has to come out of the plane perpendicular to the static magnetic field, which appears very likely to happen. Otherwise the decay process is extremely slow due to the topological constraint [see, V. P. Mineyeev and G. E. Volovik, Phys. Rev. B 18, 3197 (1978)].

[10]K. Maki, in *Quantum Fluids and Solids,* edited by S. B. Trickey, E. D. Adams, and J. W. Dufty (Plenum, New York, 1977).

[11]A. Barone, F. Esposito, C. J. Magee, and A. C. Scott, Riv. Nuovo Cimento 1, 227 (1977).

[12]See, for example, in *Handbook of Mathematical Functions,* edited by M. Abramowitz and I. A. Stengun (Dover, New York, 1965), Chap. 16.

[13]H. Smith, W. F. Brinkman, and S. Engelesberg, Phys. Rev. B 15, 199 (1977).

[14]We are indebted to Dieter Vollhardt for providing us more accurate values for λ_f and λ_g for the splay composite soliton

[15]W. F. Brinkman and H. Smith, Phys. Lett. A 53, 43 (1975).

[16]M. C. Cross and P. W. Anderson, in *Proceedings of the XIV International Conference on Low Temperature Physics, Otaniemi, Finland, 1975,* edited by M. Krusius and M. Vuorio (North-Holland, Amsterdam, 1975), Vol. 1, p. 29.

[17]K. Maki, J. Low Temp. Phys. 32, 1 (1978).

[18]D. N. Paulson, M. Krusius, and J. C. Wheatley, Phys. Rev. Lett. 22, 1322 (1976).

[19]M. Krusius, D. N. Paulson, and J. C. Wheatley, J. Low Temp. Phys. 33, 255 (1978).

[20]E. Merzbacher, *Quantum Mechanics* (Wiley, New York, 1961), Chap. 6.

[21]L. D. Landau and E. M. Lifshitz, *Quantum Mechanics* (Pergamon, Oxford, 1969).